Available online at www.sciencedirect.com

SCIENCE DIRECT®

Thermochimica Acta 427 (2005) 193–200

thermochimica acta

www.elsevier.com/locate/tca

Thermal analysis and temperature-programmed reduction studies of copper–zirconium and copper–zirconium–yttrium compounds

Madona Labaki[1], Jean-François Lamonier*, Stéphane Siffert, Antoine Aboukaïs

Laboratoire de Catalyse et Environnement, E.A. 2598, MREI, Université du Littoral - Côte d'Opale, 145,
Avenue Maurice Schumann, 59140 Dunkerque cedex, France

Received 27 May 2004; received in revised form 27 August 2004; accepted 13 September 2004

Abstract

Differential thermal analysis evidenced that introduction of copper or yttrium into zirconia matrix delays its crystallization temperature. This result was connected to the stabilization of the zirconia tetragonal phase observed by X-ray diffraction. In addition, it was observed a decomposition delay of supported copper nitrate with yttrium content in a zirconia support. Temperature-programmed reduction revealed the existence of different copper species: isolated copper ions, copper clusters, small particles of copper oxide and bulk copper oxide. The reduction temperature of these species was strongly influenced by the preparation method of Cu–Zr systems and by the presence of yttrium in ZrO_2. But in all the samples, isolated copper ions and clusters were postulated to be reduced at the same temperature since these species have the same electron paramagnetic resonance parameters and then occupy the same sites. A correlation was done between the reducibility of these copper species and their activity in propene and toluene oxidation reactions. In the absence of yttrium, the best activity measured was correlated to an easier reduction but also to a higher quantity of isolated copper ions and clusters. Addition of yttrium to the support modified the copper interaction. At low copper/zirconium atomic ratio (0.01), the reduction temperature of small CuO particles increased with the yttrium content in the support. At high copper content (Cu/Zr = 0.1), the easier copper species reduction was obtained for Y_2O_3 content of 5 wt.%, the corresponding solid providing the best activity in the propene oxidation.

Keywords: DTA-TG; H_2-TPR; Copper–zirconium; Copper–zirconium–yttrium

1. Introduction

The problem to diminish the amount of harmful industrial and automotive emissions (such as VOCs, diesel soot, NO_x, etc.) is one of the most actual problems. Different methods could be used for this aim. The catalytic oxidation was proposed because of the controlled selectivities that might be obtained, the low cost of the necessary materials and low energy consumption. The choice of oxide catalysts was claimed for catalytic oxidation, since a mechanism was proposed where the oxygen of the oxide is involved in the oxidation and is substituted by the oxygen of the phase gas [1–3]. Zirconium dioxide or zirconia (ZrO_2) is an interesting material used in oxidation catalysis. Lability and easiness to exchange oxygen atoms of the tetragonal or cubic ZrO_2 phase make them suitable for redox catalysis [4,5]. In our previous study [6], different samples zirconia modified by copper synthesized according to different preparation modes were characterized and tested in propene complete oxidation reaction. In another article from our group [7], different zirconia–yttria supports were characterized and tested towards propene and toluene deep oxidation reactions before and after copper impregnation. A difference in the catalytic behaviour was measured between these different studied samples. The present paper will focus on the thermal behaviour of these different samples under oxidizing and reducing atmosphere. Indeed the stability of the support zirconia and the interaction of the cop-

---

* Corresponding author. Tel.: +33 3 28 65 82 56; fax: +33 3 28 65 82 39. *E-mail address:* lamonier@univ-littoral.fr (J.-F. Lamonier).

[1] Present address: Faculté des Sciences II, Université Libanaise, Fanar El-Metn, Liban, Lebanon.

0040-6031/$ – see front matter © 2004 Elsevier B.V. All rights reserved.
doi:10.1016/j.tca.2004.09.013

per species with the support can be followed by differential thermal analysis (DTA) combined to a simultaneous thermogravimetric analysis (TG). Since the activity of oxide catalysts towards total oxidation reactions is mainly correlated to the reducibility of the active species [8–12], temperature-programmed reduction (TPR) of the copper samples has been investigated. Copper could be present in different forms on the support surface depending on the amount of deposited copper and on the support properties:

- isolated copper species Cu^{2+} with strong interaction with the support [5,11,13];
- Cu^{2+} clusters dispersed on the solid surface [11,13,14];
- highly dispersed CuO particles also designated by small particles of CuO [15];
- big aggregates of CuO also known as bulk CuO [5,13,15–18].

TPR allows a fine analysis of the different copper species present in the solids since, in this technique, each copper species has its own reduction peak. However, the interpretation of the TPR peaks is not always evident and the peaks assignments remain a subject of debate.

Therefore, the goal of the present work is to make clear DTA-TG and TPR results with the help of our previous studies [6,7]. The work will be divided into two parts: the first one will consist on the influence of the preparation mode of the copper–zirconium samples studied in the Ref. [6] and the second one will report the influence of the support type in the samples of copper supported zirconia–yttria studied in the Ref. [7]. In each part, two copper atomic ratios with Cu/Zr = 0.01 and 0.1 are investigated.

2. Experimental

2.1. Samples preparation

Copper–ZrO_2 samples were synthesized by three different methods: coprecipitation of copper and zirconium, impregnation of copper over zirconium oxyhydroxide and impregnation of copper over zirconium oxyhydroxide previously calcined at 600 °C (zirconium dioxide). For the coprecipitated samples, appropriate amounts of copper nitrate trihydrate $Cu(NO_3)_2\cdot 3H_2O$ (PROLABO, purity $\geq$99.9%) and zirconium oxychloride octahydrate $ZrOCl_2\cdot 8H_2O$ were dissolved in deionized water. This solution was added to an excess of ammonia solution $NH_3\cdot H_2O$ 0.7 M. The resultant coprecipitate was filtered, washed, dried overnight at 100 °C and finally crushed. The impregnated samples were prepared by wet impregnation of appropriate amounts of copper nitrate trihydrate $Cu(NO_3)_2\cdot 3H_2O$ aqueous solution on $ZrO(OH)_2$ or ZrO_2 (previously calcined at 600 °C). Preparation details are described elsewhere [6].

All the samples were calcined at 600 °C (4 h) and designated by Cu_x–Zr600 for the coprecipitates (specific area of 80 and 40 $m^2\,g^{-1}$ for respectively $x = 0.01$ and $x = 0.1$), $Cu_x/ZrO(OH)_2600$ for the samples copper impregnated over zirconium oxyhydroxide (100 $m^2\,g^{-1}$) and by Cu_x/Zr600/600 for the samples copper impregnated over zirconium dioxide (70 $m^2\,g^{-1}$), where x = Cu/Zr designates the atomic ratio in the sample ($x = 0.01$ and 0.1).

Yttrium was introduced into zirconia matrix as a stabilizer of zirconia tetragonal phase, zirconia crystalline phase known to be catalytically active in oxidation reactions [4,19]. Tetragonal solid solutions of ZrO_2–Y_2O_3 calcined at 600 °C were impregnated by copper cations (using copper nitrate solution) with the subsequent drying at 100 °C (24 h) and calcination at 450 °C (4 h). Synthesis details are reported elsewhere [7]. The solids were denoted by Cu_x/Zr-aY600, where x represents the Cu/Zr atomic ratios of 0.01 and 0.1 and a the molar percentage of yttrium in the support (a = 1, 5 and 10).

2.2. Characterization methods

Differential thermal analysis and thermo-gravimetric analysis (DTA-TG) experiments of the samples before calcination were carried out in air (75 mL/min) at a heating rate of 5 °C/min till 700 °C with a Netzsch STA 409 C instrument equipped with a microbalance and a gas flow system. About 45 mg of sample were used for each analysis.

Temperature-programmed reduction (TPR) of the calcined solids was carried out in a conventional laboratory apparatus (Zeton Altamira AMI 200) consisting of a gas supply system with mass-flow controllers, a quartz U-reactor, a water vapour trap and a thermal conductivity detector (TCD). The sample bed temperature was monitored with a thermocouple protected by a quartz tube inserted in the centre of the sample bed with its tip located a few millimetres above the sample bed. In order to minimize the contribution of adsorbed species to the TPR profiles, prior to the TPR experiments all samples were pretreated in argon at 150 °C for 1 h. The samples were heated from ambient to 600 °C under H_2 (5 vol.% in argon) flow (30 mL/min) at a heating rate of 5 °C/min.

3. Results and discussion

3.1. Influence of the preparation mode

DTA experiments (Fig. 1) of the different copper–zirconium samples show the existence of one exothermic peak. This peak is not accompanied by any significant mass loss (TG curves not shown) and is attributed to the crystallization into the tetragonal phase of ZrO_2 containing copper. This crystallization phenomenon occurring at 420 °C for pure zirconium oxide [20] is delayed when copper was present in the solid.

For the same type of preparation, the crystallization delay is enhanced with increasing copper content. Furthermore, for the same copper content in different preparations, the crystallization is more delayed in the following order:

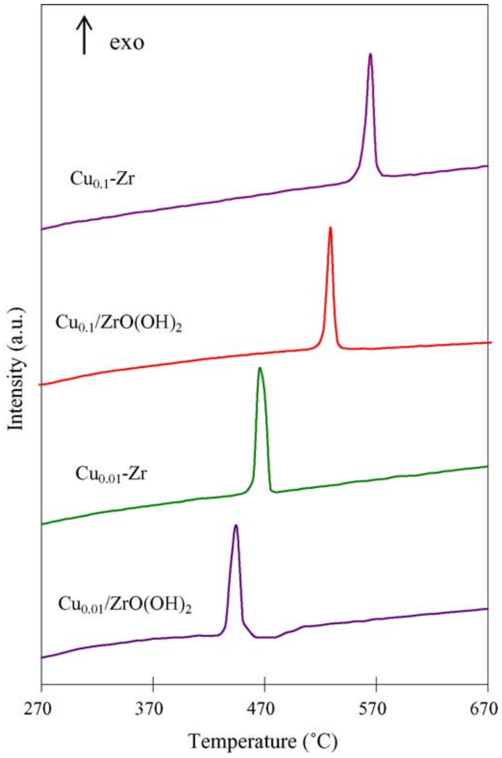

Fig. 1. DTA curves obtained during the calcination under air (75 mL/min) of the different copper and zirconium-based samples (45 mg).

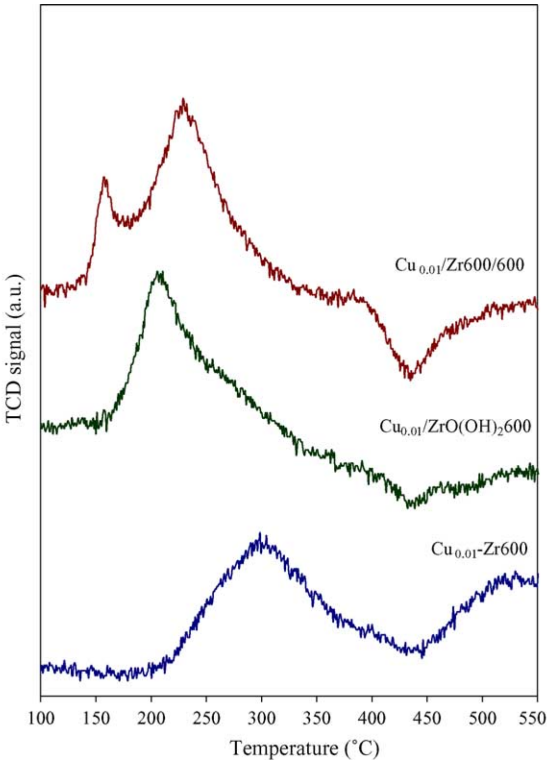

Fig. 2. H_2-TPR profiles of copper–zirconium samples with Cu/Zr ratio of 0.01.

copper/$ZrO(OH)_2$ < coprecipitates Cu–Zr. Thus, it seems that the more the quantity of copper in the bulk, the more is the crystallization delay. Therefore, for $Cu_x/ZrO(OH)_2$ and Cu_x–Zr samples calcined at the same temperature (600 °C), the degree of crystallisation is probably different. The weak crystallization of the coprecipitate could be responsible for the higher distortion of copper octahedral site observed by electron paramagnetic resonance (EPR) [6]. The delay of crystallization could be also connected to the XRD results: a stabilization of the tetragonal phase of zirconia at room temperature has been observed when copper is mainly present in the bulk of the solid ($Cu_x/ZrO(OH)_2$ and Cu_x–Zr) whereas a mixture of monoclinic and tetragonal phases has been detected for Cu_x/ZrO_2 sample [6].

TPR profiles of copper–zirconium samples synthesized by three different methods with Cu/Zr atomic ratio = 0.01 (Fig. 2) show at low temperature one reduction peak respectively at 302 and 210 °C for $Cu_{0.01}$–Zr600 and $Cu_{0.01}/ZrO(OH)_2600$ and show two reduction peaks respectively at 160 and 232 °C for $Cu_{0.01}$/Zr600/600. Besides, a negative TPR peak at about 440 °C is clearly observed for the impregnated samples. It is noteworthy to say that pure zirconia calcined at 600 °C does not show any reduction peak in TPR in our conditions. This fact was also observed in the works of Zhou et al. [15]. But when copper is present in the bulk ($Cu_{0.01}$–Zr), an additional H_2 consumption is observed at around 520 °C. This signal can be attributed to the initial reduction of ZrO_2, made easier when copper is well dispersed in the bulk of this oxide.

In EPR, two types of copper species have been evidenced for the three samples [6]: isolated copper ions and copper clusters. So, the large reduction peak observed for $Cu_{0.01}$/Zr600/600, $Cu_{0.01}/ZrO(OH)_2600$ and $Cu_{0.01}$–Zr600 could be ascribed to the reduction of these species. These species reductions are supposed to occur at closed temperature since in our previous study [6], isolated copper ions and clusters have been found to have, in a given sample, the same EPR parameter g_{iso} because they might occupy the same type of sites. The reduction temperature is higher in the case of the coprecipitate because copper is rather present in the solid bulk and then is less accessible. Comparing the both impregnated samples, the reduction occurs at higher temperature for $Cu_{0.01}$/Zr600/600 than for $Cu_{0.01}/ZrO(OH)_2600$ sample. This could be explained by the difficulty faced by hydrogen to access the copper species because of the lower specific surface area of $Cu_{0.01}$/Zr600/600 [6], which leads to a more difficult accessibility of H_2 in order to reduce the copper present on the surface. Taking into account the sintering of copper by the calcination at 600 °C after impregnation, one could put forward that some quantity of copper oxide is formed, which is supposed to be under the form of small particles of CuO or of bulk copper oxide. XRD results showed that bulk CuO was not observed in our three samples. Moreover, Shimokawabe et al. [21] have found that for Cu/ZrO_2 systems, with copper loadings below 1 wt.%, no bulky CuO has been detected when these samples have been calcined at 300–700 °C. So the low content of copper in our samples (Cu/Zr atomic ratio of 0.01 corresponds to about 0.5 wt.% of Cu) explains the absence of bulk CuO. But we cannot exclude the formation of small particles of CuO since XRD and EPR measurements cannot evidence such species. The decrease of the effective intensity of the isolated Cu^{2+} EPR signal measured for $Cu_{0.01}$/Zr600/600 sample in comparison with the other samples, suggests the possible formation of non-visible copper species as small particles of CuO in this solid. This hypothesis is strengthened by the lower BET value of $Cu_{0.01}$/Zr600/600 [6], which leads to a lower copper species dispersion.

It is well known that the small CuO particles are more easily reduced than isolated copper and clusters because of their weaker interaction with the support [5,11,13,21]. Hence, the TPR peak observed at 160 °C for $Cu_{0.01}$/Zr600/600 could be ascribed to reduction of small particles of CuO.

Moreover, the presence of the negative TPR peak (at 440 °C) could be explained by the hydrogen trapping. Indeed, owing to both the dynamical situation, caused by the large fractional H_2 consumption, and to the H_2 (or H_2O) adsorption–desorption phenomena, Fierro et al. [22] have observed a double peak instead of a one single peak in the reduction profiles of CuO and Cu_2O, which was attributed to the desorption of hydrogen trapped by the solid.

The different TPR curves of copper zirconium samples with Cu/Zr = 0.1 are depicted in Fig. 3. In the profiles of $Cu_{0.1}$–Zr600, $Cu_{0.1}$/$ZrO(OH)_2$600 and $Cu_{0.1}$/Zr600/600, a peak at ∼156 °C is observed with a shoulder at ∼150 °C, a second peak is observed at 208 °C for $Cu_{0.1}$/$ZrO(OH)_2$600 and $Cu_{0.1}$/Zr600/600 and scarcely observed at 230 °C for $Cu_{0.1}$–Zr600. Moreover, a negative peak is observed in the range 415–430 °C for $Cu_{0.1}$/$ZrO(OH)_2$600 and $Cu_{0.1}$/Zr600/600. As previously mentioned, this peak could be assigned to the release of hydrogen trapped in the solid. TPR profile of the simple mechanical mixture mmCuO + Zr600 (Cu/Zr = 0.1) is composed of one reduction peak located at 278 °C. The single reduction peak observed for mmCuO + Zr600 can be unambiguously attributed to bulk CuO reduction since this species is the lone type of copper species evidenced in this sample.

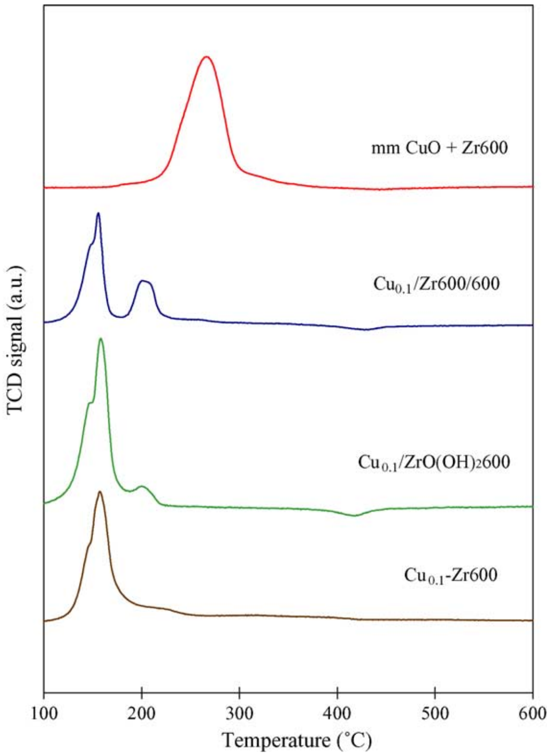

Fig. 3. H_2-TPR profiles of copper–zirconium samples with Cu/Zr ratio of 0.1.

The intensity of the second TPR peak which is observed at around 210 °C for the impregnated samples and at 230 °C for the coprecipitate decreases in the following order: $Cu_{0.1}$/Zr600/600, $Cu_{0.1}$/$ZrO(OH)_2$600 and $Cu_{0.1}$–Zr600. This peak could be assigned to bulk CuO reduction. Indeed, XRD analysis revealed the presence of bulk copper oxide for the sample $Cu_{0.1}$/Zr600/600 [6], according to the higher probability to form these species on a lower specific area. The lower signal intensity for $Cu_{0.1}$/$ZrO(OH)_2$600 and $Cu_{0.1}$–Zr600 indicates probably a lower proportion of bulk CuO which cannot be observed by XRD due to the detection limit of this technique.

The maximum temperature of bulk copper oxide reduction peak for the three samples is lower than that of bulky CuO in the mmCuO + Zr600 sample and can be explained by a change in the CuO dispersion under the influence of the support. Some copper interaction with the support should exist and therefore could enhance bulk copper oxide reduction in the samples prepared by the as-described three methods.

By EPR, in Cu/Zr = 0.1 samples, isolated copper ions and copper clusters was always observed. However, the resolution of the hyperfine structure was lower than that of the samples with Cu/Zr = 0.01, fact that indicates a lower amount of isolated copper ions and consequently a higher amount of the other types of copper species like CuO species previously described.

The shoulder at 150 °C could be due to small CuO particles reduction. The presence of these species in the samples is suggested because they are intermediates between copper clusters whose EPR signal is observed and bulk copper oxide, which is present in the samples. The TPR peak at 156 °C could be due to isolated copper and copper clusters simultaneous reduction. It might be suggested that the latter reduction begins to occur before the end of small CuO particles reduction.

It should be remarked that the reduction temperature of isolated copper species and clusters is of 302 °C for $Cu_{0.01}$–Zr600, of 210 °C for $Cu_{0.01}$/$ZrO(OH)_2$600 and of 232 °C for $Cu_{0.01}$/Zr600/600 while it is of 156 °C for $Cu_{0.1}$–Zr600, $Cu_{0.1}$/$ZrO(OH)_2$600 and $Cu_{0.1}$/Zr600/600. For enough copper content (Cu/Zr = 0.1), the support seems not to play a role in the reduction of isolated copper species and clusters since the temperature required for this reduction is the same. H_2 activation on the surface is probably the rate-limiting step of the reduction process. Soczyski et al. [23], studying the reduction kinetics of CuO in $CuO/ZnO/ZrO_2$ systems, found that the reduction of CuO is an autocatalytic consecutive reaction. This autocatalytic effect is due to facilitated dissociation of H_2 on the metallic copper formed [23]. In this condition, the formation of metallic copper at the beginning of the reduction can enhance the reduction of the remaining copper species. This can explain a lower reduction temperature of isolated copper species and clusters for Cu/Zr = 0.1 samples. This phenomenon is not observed for Cu/Zr = 0.01 samples. Indeed for $Cu_{0.01}$/Zr600/600, the presence of small CuO particles does not improve isolated copper and clusters reduction in comparison with isolated copper and clusters reduction observed in $Cu_{0.01}/ZrO(OH)_2600$ and $Cu_{0.01}$–Zr600 samples (Fig. 2). This result is explained by the copper content in the sample, which is too low (0.5 wt.%) to significantly contribute to the decrease of reduction temperature of isolated copper species and clusters.

In our previous study [6], whatever the copper content, the following order of catalytic activity in total propene oxidation was observed: Cu–Zr600 < Cu/Zr600/600 ≤ $Cu/ZrO(OH)_2600$.

The lower activity of the coprecipitated catalysts in comparison with the impregnated ones is expected according to the synthesis method, which leads surely to a lower quantity of copper species at the surface. Then the attempt of correlation can be done only between the both impregnated catalysts. Supposing that hydrocarbons catalytic oxidation occurs according to a redox mechanism [1–3] the temperature of reduction but also the corresponding reduced copper quantity could be the main parameters to explain the difference in activity.

Taking into account the lack of small CuO particles for $Cu_{0.01}/ZrO(OH)_2600$ and the best activity measured for this sample, one can assume that isolated copper ions and clusters play the main role in catalytic activity. Moreover, the reduction of these latter species for $Cu_{0.01}/ZrO(OH)_2600$ takes place at lower temperature than that for $Cu_{0.01}$/Zr600/600. The easier reduction but also the higher quantity of isolated copper ions and clusters (no CuO) explain well the difference in activity.

However, for Cu/Zr = 0.1 samples, the reduction temperature of isolated copper ions and clusters is the same for the both impregnated samples. The difference in activity is then explained by the difference in isolated copper ions and clusters quantity. Indeed, TPR measurement reveals a higher proportion of these species regarding the entire copper species.

Besides, the mechanical mixture of mmCuO + Zr600 was less active in propene oxidation reaction [6] than the other catalysts. In parallel, bulk CuO in this sample is less reducible than in the other catalysts with the same copper content. Indeed, it could be inferred that CuO must have some kind of interaction with zirconia in order to be more active.

3.2. Influence of the zirconia–yttria support

The thermal decomposition of simple and mixed zirconium and yttrium hydroxides was investigated by our group in a previous study [7]. It has been shown the delay of zirconia crystallization when yttrium is introduced into its matrix. The more the yttrium content, the more the zirconia crystallization delay is. It has also been shown that the resultant oxides are tetragonal. So yttrium stabilizes the zirconia tetragonal phase and delays its crystallization. For pure yttrium hydroxide, no visible peak has been observed [7]. This has been explained by the slow crystallization of yttria.

The decomposition of copper nitrate impregnated on different zirconia–yttria supports calcined at 600 °C was here investigated. The copper nitrate decomposition as a function of zirconia–yttria supports is described in Fig. 4. An endothermic peak at about 220 °C was observed in each case. This peak can be attributed to copper nitrate decomposition because the mass loss associated to the endothermic signal corresponds to the theoretical decomposition of $Cu(NO_3)_2$ into CuO. Indeed the theoretical mass loss for the supports impregnated by 5 wt.% of copper (Cu/Zr = 0.1), that accompanies the decomposition of $Cu(NO_3)_2$ to CuO, is of about 7.7%. For the endothermic signal observed (∼220 °C), a corresponding experimental mass loss of about 7.5% was recorded. This is in accordance with some authors that have demonstrated that the calcination of copper nitrate under air leads to CuO formation [5,13,21,24]. In fact, the change of the colour of our compounds after calcination under air from blue-green (copper nitrate colour) to black (CuO colour) was observed. Moreover, the thermal analysis of an additional sample impregnated with 8 wt.% of copper (Cu/Zr = 0.17)

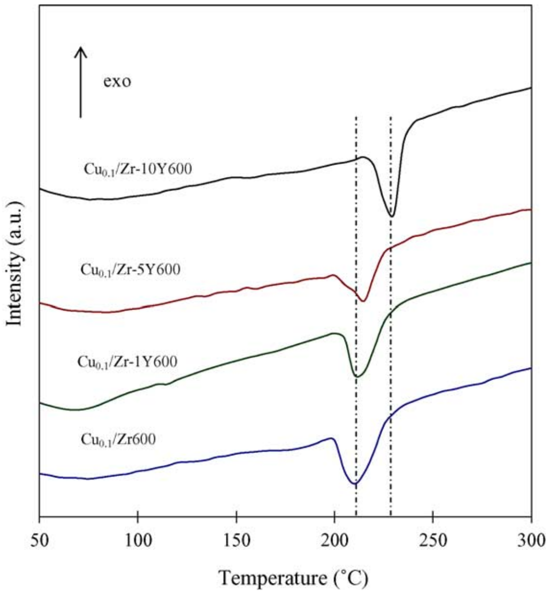

Fig. 4. DTA curves of the thermal treatment (5 °C/min) under air flow (75 mL/min) of copper nitrate impregnated on different zirconia–yttria supports (Cu/Zr = 0.1) (45 mg).

(Fig. 5) evidences the proportionality between the copper content and the mass loss associated with the endothermic peak at ∼220 °C.

However, the endothermic peak due to copper nitrate decomposition (Fig. 4) is present at a temperature of 208 °C for $Cu_{0.1}$/Zr600 and of 215, 220 and 230 °C for the samples $Cu_{0.1}$/Zr-1Y600, $Cu_{0.1}$/Zr-5Y600 and $Cu_{0.1}$/Zr-10Y600 respectively. So, it seems that the nitrate decomposition is more delayed when the yttrium content in the support increases. This effect could be explained by the important hygroscopy of yttrium which could modify copper chemical environment. Another explanation of this phenomenon could be suggested by EPR characterization where different $A_{\parallel}$ (parallel hyperfine constant) values were obtained for copper deposited on zirconia simple or mixed oxide supports and on yttria support (134 G for $Cu(NO_3)_2$/Zr600 or $Cu(NO_3)_2$/Zr-aY600 and 152 G for $Cu(NO_3)_2$/Y600). Indeed the higher $A_{\parallel}$ value obtained for copper impregnated on yttria support indicates a higher number of ligands in the neighbourhood of copper. Thus, the decomposition of the nitrate precursor requires higher temperatures.

Finally, it should be interesting to note that an endothermic peak at about 80 °C was observed and attributed to physisorbed water departure and was more important with higher yttrium content in the support, the yttrium oxide being very hygroscopic [25].

Fig. 6 displays TPR profiles of $Cu_{0.01}$/Zr-aY600 samples. Two reduction peaks are seen respectively at 164 and 207 °C for $Cu_{0.01}$/Zr-1Y600 and at 186 and 209 °C for $Cu_{0.01}$/Zr-5Y600. For $Cu_{0.01}$/Zr-10Y600 one reduction peak at 206 °C is observed. Moreover, the negative TPR peak at ∼440–450 °C is always observed.

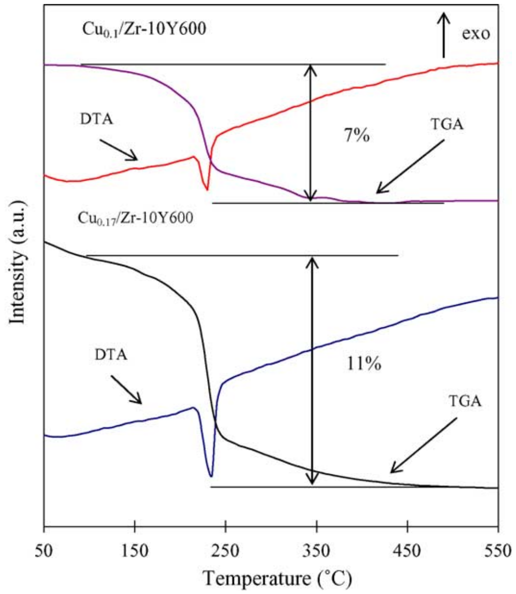

Fig. 5. DTA and TG curves of the thermal treatment (5 °C/min) under air flow (75 mL/min) of copper nitrate impregnated on Zr-10Y600 support (Cu/Zr = 0.1 and Cu/Zr = 0.17) (45 mg).

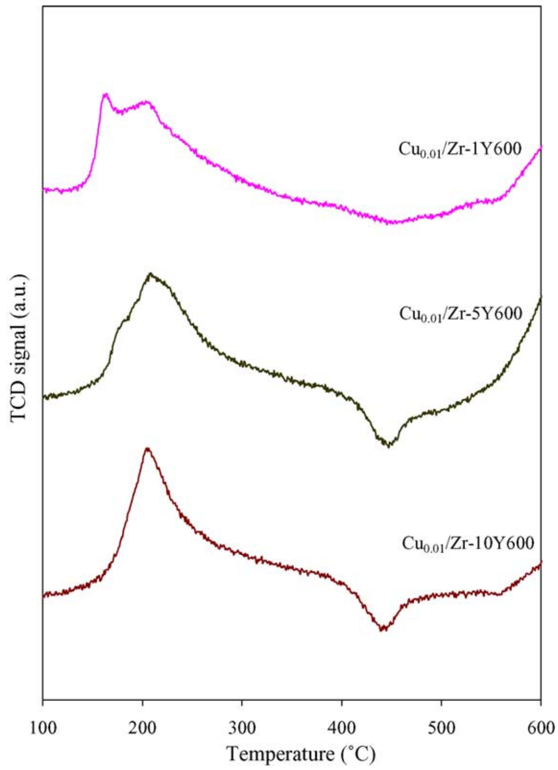

Fig. 6. H_2-TPR profiles of copper impregnated on mixed zirconia–yttria supports (Cu/Zr = 0.01).

In comparison with $Cu_{0.01}/ZrO_2$ sample, H_2-TPR signal of $Cu_{0.01}$/Zr-1Y600 is very similar. Moreover, since EPR signals of both isolated copper ions and copper clusters species were detected [7] for the different $Cu_{0.01}$/Zr-aY600 samples, the same attribution for the TPR signals can be given: at lower temperature the reduction of small CuO particles in low interaction with the support takes place whereas at higher temperature the simultaneous reduction of isolated copper ions and copper clusters occurs. Then the reduction peak observed at 164 °C for $Cu_{0.01}$/Zr-1Y600 and at 186 °C for $Cu_{0.01}$/Zr-5Y600 can be attributed to the reduction of small CuO particles. However, the more the yttrium content in the support, the more this reduction peak is delayed. For $Cu_{0.01}$/Zr-10Y600, the reduction peak of small CuO particles takes place at the same temperature than that of isolated copper ions and copper clusters. Concerning the reduction of both isolated copper ions and copper clusters species, it seems that yttrium content in the sample does not significantly influence the reduction temperature (around 210 °C for $Cu_{0.01}$/Zr-aY600). But in comparison with $Cu_{0.01}/ZrO_2$ sample the reduction of this species takes place at lower temperature (around 230 °C for $Cu_{0.01}/ZrO_2$ sample). This result indicates that dispersion of copper species is quite different on pure ZrO_2 than on Zr-aY_2O_3 support and can be explained by different specific surface area values ($ZrO_2 \sim 70\ m^2\ g^{-1}$ and Zr-a$Y_2O_3 \sim 90–95\ m^2\ g^{-1}$) [7]. Moreover, the catalytic oxidation of propene and toluene investigated on these samples

[7] has revealed that $Cu_{0.01}$/Zr-aY600 solid presents a higher activity than that measured in the presence of $Cu_{0.01}/ZrO_2$. So the easier reduction of copper species in the case of $Cu_{0.01}$/Zr-aY600 can be connected to the best catalytic results observed with these catalysts. The comparison of the TPR profiles of Cu/Zr-aY600 allows also making clear the difference of catalytic activity observed in the Cu/Zr-aY600 samples [7]. Indeed, although mixed oxides Zr-aY600 samples have similar specific surface area values, the copper interaction with the support is affected by the yttrium content. Besides, the increase of copper species interaction with yttrium content in the support was previously evidenced by differential thermal analysis of copper nitrates decomposition.

TPR profiles of the different $Cu_{0.1}$/Zr-aY600 samples are shown in Fig. 7. TPR pattern of $Cu_{0.1}$/Zr-1Y600 is very similar to that obtained with $Cu_{0.1}$/Zr600: the first reduction peak is due to reduction of small CuO particles, the second one to the simultaneous reduction of isolated copper ions and clusters and the third one can be ascribed to bulk copper oxide reduction.

The presence of higher yttrium content ($Cu_{0.1}$/Zr-5Y600) leads to analogous TPR profiles but at lower temperature an additional shoulder is observed. Moreover, the contribution of isolated copper ions and clusters decreases to the benefit of bulk CuO contribution. This result is in good correlation with EPR measurement, which reveals for this sample a lower quantity of Cu^{2+} paramagnetic species (isolated copper ions and clusters) in comparison with that observed for $Cu_{0.1}$/Zr-1Y600 [7].

Addition of higher yttrium content in the support ($Cu_{0.1}$/Zr-10Y600) modifies the TPR profile since higher temperatures are required to reduce all the copper species. The first peak should be due to the reduction of isolated copper ions and clusters since EPR spectrum of this sample presents the same relative quantity of Cu^{2+} paramagnetic species than that observed for $Cu_{0.1}$/Zr-1Y600 solid. The presence of small particles of CuO in this sample cannot be excluded since these species are intermediate between isolated copper ions and clusters from one part and bulk copper oxide from the other. It is assumed that small copper oxide particles and isolated copper ions and clusters are reduced at the same temperature.

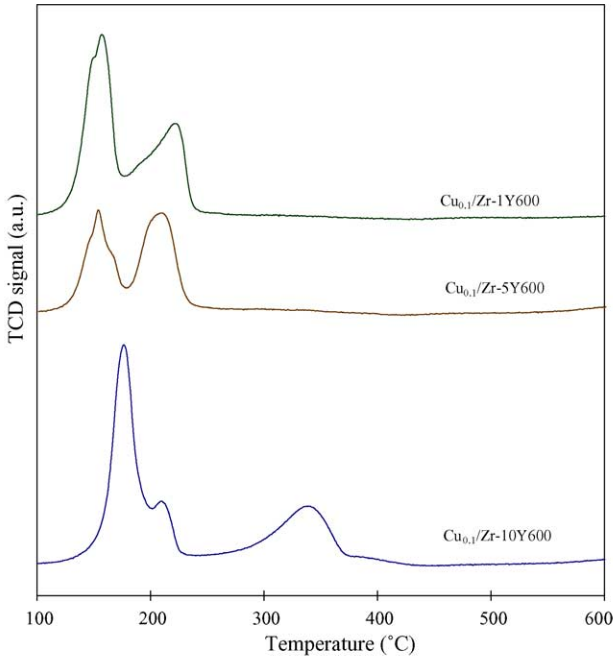

Fig. 7. H_2-TPR profiles of copper impregnated on mixed zirconia–yttria supports (Cu/Zr = 0.1).

The peaks at 214 and 343 °C are probably related to the reduction of bulk copper oxide in different environments. The first one should correspond to the reduction of bulk CuO in interaction with ZrO_2, in view of the fact that the same temperature of CuO reduction is observed with pure zirconia and oxides with low yttrium content (Zr-1Y600, Zr-5Y600). The second one should be then attributed to bulk CuO in interaction with Y_2O_3, a similarity with the TPR patterns of copper on yttria supports (not presented here) was observed.

The catalytic activity of $Cu_{0.1}$/Zr-aY600 in propene and toluene deep oxidation reactions follows the order: $Cu_{0.1}$/Zr-10Y600 < $Cu_{0.1}$/Zr-1Y600 ≤ $Cu_{0.1}$/Zr-5Y600 [7]. The catalytic behaviour is in line with the TPR results and especially with the reducibility of copper species. Indeed the lowest activity measured for $Cu_{0.1}$/Zr-10Y600 is well explained by higher reduction temperature of copper species. The slight increase of activity observed for $Cu_{0.1}$/Zr-5Y600 catalyst compared with that for $Cu_{0.1}$/Zr-1Y600 could be explained by the presence of copper species reducible at lower temperature.

4. Conclusion

Different copper–zirconia and copper–zirconia–yttria solids were characterized by DTA-TG and TPR. DTA-TG studies reported a delay of zirconia crystallization when copper or yttrium was introduced into its lattice. In addition, for the samples copper deposited on zirconia–yttria supports, the endothermic peak corresponding to copper nitrate degradation shifted to higher temperatures with the increase of yttrium content. The different chemical environment of copper into the solid could explain the delay of copper nitrate decomposition into copper oxide.

TPR patterns were found to reflect the states of copper-based samples. TPR patterns of the different copper–zirconia samples synthesized by different methods reveal the presence of small copper oxide particles, which are more reducible than isolated copper ions and clusters. These latter species are found to be reduced at the same temperature because of their same electron paramagnetic resonance parameters. The less reducible bulk copper oxide species was evidenced for the samples with Cu/Zr = 0.1. TPR results were in line with catalysts activity towards propene deep oxidation reaction; it was suggested that the catalysts activity towards this reaction is mainly due to the amount of isolated copper ions and clusters and/or to the reducibility of these species. Moreover, it was postulated that some interaction between bulk copper oxide and the support is required for a better catalytic activity.

For the samples copper impregnated on zirconia and mixed zirconia–yttria supports, TPR evidenced the presence of isolated copper ions and copper clusters besides small particles of CuO. These species are probably reduced at the same temperature in the samples Cu_x/Zr-10Y. Bulk copper oxide species was evidenced for the samples with Cu/Zr = 0.1. The correlation between copper species reducibility and catalysts activity towards propene and toluene total oxidation reactions was underlined; the samples whose copper species are more easily reduced present higher catalytic activities.

Acknowledgements

The conseil général du Nord, the region Nord-Pas de Calais and the European community are gratefully acknowledged for financial supports.

References

[1] S. Minicò, S. Scirè, C. Crisafulli, A.M. Visco, S. Galvagno, Appl. Catal. B 28 (2000) 245–251.
[2] M. Baldi, E. Finocchio, F. Milella, G. Busca, Appl. Catal. B 16 (1998) 43–51.
[3] E.M. Cordi, P.J. O'Neill, J.L. Falconer, Appl. Catal. B 14 (1997) 23–36.
[4] A. Martinez-Arras, M. Fernàndez-Garcia, C. Belver, J.C. Conesa, J. Soria, Catal. Lett. 65 (2000) 197–204.
[5] W.-P. Dow, Y.-P. Wang, T.-J. Huang, J. Catal. 160 (1996) 155–170.
[6] M. Labaki, J.F. Lamonier, S. Siffert, E.A. Zhilinskaya, A. Aboukaïs, Colloid Surf. A 227 (2003) 63–75.
[7] M. Labaki, S. Siffert, J.F. Lamonier, E.A. Zhilinskaya, A. Aboukaïs, Appl. Catal. B 43 (2003) 261–271.
[8] L. Zanderighi, M.P. Faedda, S. Carrà, J. Catal. 35 (1974) 427–433.
[9] Y. Morooka, A. Ozaki, J. Catal. 5 (1966) 116–122.
[10] I. Aso, M. Nakao, N. Yamazoe, T. Seiyama, J. Catal. 57 (1979) 287–295.
[11] Lj. Kundakovic, M. Flytzani-Stephanopoulos, Appl. Catal. A 171 (1998) 13–29.
[12] M.M. Günter, T. Ressler, R.E. Jentoft, B. Bems, J. Catal. 203 (2001) 133–149.
[13] S.P. Kulyova, E.V. Lunina, V.V. Lunin, B.G. Kostyuk, G.P. Muravyova, A.N. Kharlanov, E.A. Zhilinskaya, A. Aboukaïs, Chem. Mater. 13 (2001) 1491–1496.
[14] G. Centi, G. Cerrato, S. D'Angelo, U. Finardi, E. Giamello, C. Morterra, S. Perathoner, Catal. Today 27 (1996) 265–270.
[15] R. Zhou, T. Yu, X. Jiang, T. Chen, X. Zheng, Appl. Surf. Sci. 148 (1999) 263–270.
[16] Y. Hu, L. Dong, J. Wang, W. Ding, Y. Chen, J. Mol. Catal. A: Chem. 162 (2000) 307–316.
[17] L. Ma, M.-F. Luo, S.-Y. Chen, Appl. Catal. A 242 (2003) 151–159.
[18] J. Xiaoyuan, L. Guanglie, Z. Renxian, M. Jianxin, C. Yu, Z. Xiaoming, Appl. Surf. Sci. 173 (2001) 208–220.
[19] G.L. Markaryan, L.N. Ikryannikova, G.P. Muravieva, A.O. Turakulova, B.G. Kostyuk, E.V. Lunina, V.V. Lunin, E. Zhilinskaya, A. Aboukaïs, Colloid Surf. A 151 (1999) 435–447.
[20] J. Matta, J.F. Lamonier, E. Abi-Aad, E.A. Zhilinskaya, A. Aboukaïs, Phys. Chem. Chem. Phys. 1 (1999) 4975–4980.
[21] M. Shimokawabe, H. Asakawa, N. Takezawa, Appl. Catal. 59 (1990) 45–58.
[22] G. Fierro, M. Lo Jacono, M. Inversi, P. Porta, R. Lavecchia, F. Cioci, J. Catal. 148 (1994) 709–721.
[23] J. Soczyski, R. Grabowski, A. Kozowska, P.K. Olszewski, J. Stoch, Phys. Chem. Chem. Phys. 5 (20) (2003) 4631–4640.
[24] V. Indovina, M. Occhiuzzi, D. Pietrogiacomi, S. Tuti, J. Phys. Chem. B 103 (1999) 9967–9977.
[25] D.R. Lide, Handbook of Chemistry and Physics, 77th ed., 1996–1997, ISBN 0-8493-0477-6.